PHILOSOPHICAL TRANSACTIONS OF THE ROYAL SOCIETY A
MATHEMATICAL, PHYSICAL & ENGINEERING SCIENCES

Experimental Results from the TFTR Tokamak

R. J. Hawryluk, V. Arunasalam, J. D. Bell, M. G. Bell, M. Bitter, W. R. Blanchard, F. Boody, N. Bretz, R. Budny, C. E. Bush, J. D. Callen, J. L. Cecchi, S. Cohen, R. J. Colchin, S. K. Combs, J. Coonrod, S. L. Davis, D. Dimock, H. F. Dylla, P. C. Efthimion, L. C. Emerson, A. C. England, H. P. Eubank, R. Fonck, E. Fredrickson, R. J. Goldston, L. R. Grisham, B. Grek, R. Groebner, H. Hendel, K. W. Hill, D. L. Hillis, E. Hinnov, S. Hiroe, R. Hulse, H. Hsuan, D. Johnson, L.-C. Johnson, R. Kaita, R. Kamperschroer, S. M. Kaye, S. Kilpatrick, H. Kugel, P. H. LaMarche, R. Little, C. H. Ma, D. M. Manos, D. Mansfield, R. T. McCann, M. McCarthy, D. C. McCune, K. McGuire, D. M. Meade, S. S. Medley, S. L. Milora, D. R. Mikkelsen, W. Morris, D. Mueller, M. Murakami, E. Nieschmidt, D. K. Owens, V. K. Pare, H. Park, B. Prichard, A. Ramsey, D. A. Rasmussen, M. H. Redi, A. L. Roquemore, N. R. Sauthoff, J. Schivell, G. L. Schmidt, S. D. Scott, S. Sesnic, M. Shimada, J. E. Simpkins, J. Sinnis, F. Stauffer, B. Stratton, G. D. Tait, G. Taylor, C. E. Thomas, H. H. Towner, M. Ulrickson, S. Von Goeler, R. Weiland, J. B. Wilgen, M. Williams, K. L. Wong, S. Yoshikawa, K. M. Young, M. C. Zarnstorff and S. Zweben

Phil. Trans. R. Soc. Lond. A 1987 **322**, 147-162
doi: 10.1098/rsta.1987.0044

Phil. Trans. R. Soc. Lond. A **322**, 147–162 (1987)
Printed in Great Britain

Experimental results from the TFTR tokamak

By R. J. Hawryluk, V. Arunasalam, J. D. Bell[1], M. G. Bell, M. Bitter, W. R. Blanchard, F. Boody, N. Bretz, R. Budny, C. E. Bush[1], J. D. Callen[2], J. L. Cecchi, S. Cohen, R. J. Colchin[1], S. K. Combs[1], J. Coonrod, S. L. Davis, D. Dimock, H. F. Dylla, P. C. Efthimion, L. C. Emerson[1], A. C. England[1], H. P. Eubank, R. Fonck, E. Fredrickson, R. J. Goldston, L. R. Grisham, B. Grek, R. Groebner[3], H. Hendel[4], K. W. Hill, D. L. Hillis[1], E. Hinnov, S. Hiroe[1], R. Hulse, H. Hsuan, D. Johnson, L.-C. Johnson, R. Kaita, R. Kamperschroer, S. M. Kaye, S. Kilpatrick, H. Kugel, P. H. LaMarche, R. Little, C. H. Ma[1], D. M. Manos, D. Mansfield, R. T. McCann, M. McCarthy, D. C. McCune, K. McGuire, D. M. Meade, S. S. Medley, S. L. Milora[1], D. R. Mikkelsen, W. Morris[5], D. Mueller, M. Murakami[1], E. Nieschmidt[6], D. K. Owens, V. K. Paré[1], H. Park, B. Prichard, A. Ramsey, D. A. Rasmussen[1], M. H. Redi, A. L. Roquemore, N. R. Sauthoff, J. Schivell, G. L. Schmidt, S. D. Scott, S. Sesnic, M. Shimada[7], J. E. Simpkins[1], J. Sinnis, F. Stauffer[8], B. Stratton, G. D. Tait, G. Taylor, C. E. Thomas[1], H. H. Towner, M. Ulrickson, S. Von Goeler, R. Weiland, J. B. Wilgen[1], M. Williams, K. L. Wong, S. Yoshikawa, K. M. Young, M. C. Zarnstorff and S. Zweben

Plasma Physics Laboratory, Princeton University, P.O. Box 451, *Princeton, New Jersey* 08544, *U.S.A.*

Recent experiments on TFTR have extended the operating régime of TFTR in both ohmic- and neutral-beam-heated discharges. The TFTR tokamak has reached its original machine-design specifications ($I_p = 2.5$ MA and $B_T = 5.2$ T). Initial neutral-beam-heating experiments used up to 6.3 MW of deuterium beams. With the recent installation of two additional beamlines, the power has been increased up to 11 MW. A deuterium pellet injector was used to increase the central density to 2.5×10^{20} m^{-3} in high-current discharges. At the opposite extreme, by operating at low plasma current ($I_p \sim 0.8$ MA) and low density ($\bar{n}_e \sim 1 \times 10^{19}$ m^{-3}), high ion temperatures (9 ± 2 keV) and rotation speeds (7×10^5 m s^{-1}) have been achieved during injection. In addition, plasma-compression experiments have demonstrated acceleration of beam ions from 82 to 150 keV, in accord with expectations. The wide operating range of TFTR, together with an extensive set of diagnostics and a flexible control system, has facilitated transport and scaling studies of both ohmic- and neutral-beam-heated discharges. The result of these confinement studies are presented.

Permanent addresses are:
[1] Oak Ridge National Laboratory, Oak Ridge, Tennessee 37831, U.S.A.
[2] University of Wisconsin, Madison, Wisconsin 53706, U.S.A.
[3] GA Technologies, Inc., San Diego, California 92138, U.S.A.
[4] RCA David Sarnoff Research Center, Princeton, New Jersey 08540, U.S.A.
[5] Balliol College, University of Oxford, Oxford OX1 3BJ, U.K.
[6] EG & G, Idaho, U.S.A.
[7] Japan Atomic Energy Research Institute, Japan.
[8] University of Maryland, College Park, Maryland 20742, U.S.A.

1. Introduction

The goals of the TFTR device are (1) to study reactor-grade plasmas with temperatures *ca.* 10 keV and densities *ca.* 10^{20} m^{-3}, and (2) to achieve approximate energy breakeven between the power input to and the fusion output from the plasma ($Q \sim 1$). These objectives require the application of intense neutral-beam heating with a full energy of 120 keV, and eventually tritium target plasmas. The increasingly wide operating range of TFTR has facilitated transport and scaling studies in both ohmic- and neutral-beam-heated discharges. With the installation of two additional beamlines, for a total of four, the neutral-beam power has been increased to *ca.* 11 MW and in a year will approach its design goal of 27 MW. The focus of the next series of experiments will be to optimize the plasma performance at these higher power levels in preparation for a demonstration in 1987 of $Q \sim 1$ equivalent conditions in deuterium discharges.

Two principal approaches exist for demonstrating $Q \sim 1$ in TFTR. The first is in the standard neutral-beam heating régime ($\bar{n}_e \gtrsim 5 \times 10^{19}$ m^{-3}, where $\bar{n}_e$ is the line-averaged density) at full power. In this régime, beam-target and thermonuclear reactions predominate. Achieving $Q \sim 1$, in this régime, will require energy confinement times of *ca.* 300 ms at full heating power (Eubank *et al.* 1985). The second is the energetic-ion régime in which beam–beam and beam–target reactions dominate. This is a low-density régime in which the energy stored in the fast ions is relatively large and the $n_e \tau_E$ required to achieve $Q \sim 1$ can be reduced significantly (Jassby 1976). Yet another alternative is to supplement neutral-beam heating with adiabatic compression by rapidly reducing the major radius. Adiabatic compression not only increases the plasma density and temperature but also increases the fast-ion energy and thus the plasma reactivity.

In this paper, a brief description of the device and the present status will be given. The operating region for ohmic- and neutral-beam-heated discharges will be described, followed by a description of parametric scaling studies of ohmically heated discharges. Neutral-beam heating, scaling and profile studies in the standard régime ($\bar{n}_e \gtrsim 3 \times 10^{19}$ m^{-3} for $P_{inj} \lesssim 11$ MW) will be discussed. A brief review of adiabatic compression results will be given, followed by a discussion of novel observations in the energetic-ion régime.

2. Machine status

TFTR is a circular tokamak with an air-core transformer. The resistance of the vacuum vessel is relatively high (3.1 mΩ) to accommodate major-radius compression experiments. A flexible control and power supply system facilitates exploration of a wide range of different operating régimes. Feedback systems are used to control the plasma current, major radius, vertical displacement, and electron density (Hawryluk *et al.* 1984; Mueller *et al.* 1986). A description of the diagnostics is given by Johnson & Young (1983).

An initial series of experiments with two neutral beamlines was completed in April 1985, during which TFTR reached its original machine design specifications in plasma current and toroidal field ($I_p = 2.5$ MA and $B_T = 5.2$ T). Subsequently, major upgrades to the neutral-beam-heating system and vacuum-vessel components have taken place.

The neutral-beam injection system was composed of two beamlines operating at *ca.* 80 kV, both injecting tangentially in the direction of the plasma current (co-injection). The maximum power, with deuterium beams, was 6.3 MW with a pulse duration of 0.5 s. Subsequently, two

PHILOSOPHICAL TRANSACTIONS OF THE ROYAL SOCIETY A MATHEMATICAL, PHYSICAL & ENGINEERING SCIENCES

additional beamlines were installed. Of these, one beamline is in the direction of the plasma current and one opposite (counter-injection). A summary of the neutral-beam system parameters is given in table 1. The tangency radii of the different beam sources were chosen to vary from 1.74 to 2.84 m to facilitate profile studies of neutral-beam power deposition. At a fixed plasma position, it is possible to select beams to heat preferentially the plasma core or the plasma edge. This capability will facilitate detailed studies to test various transport models

Table 1. Neutral beam system parameters

	April 1985	February 1986	April 1987
pulse length/s	0.5	0.5	2.0
voltage/kV	80	80	120
number of beamlines	2	4	4
ion sources	6	11	12
beamline configuration	2-co	3-co 1-counter	3-co 1-counter
power/MW (deuterium)	6.3	11	27
power at full energy	3	5.5	20

as discussed below. At the end of 1986, the beam system will be modified to provide particles with higher average energy and longer pulse duration as shown in table 1.†

Before April 1985, the major internal vacuum-vessel components were the moveable limiter assembly, bellows cover plates, and a partial set of protective plates to guard against damage to the wall of the vacuum vessel by neutral-beam power deposition. During that run, the plasma was principally limited by the moveable limiter assembly composed of three water-cooled Inconel blades covered with graphite tiles. For the large plasma experiments, the plasma major radius, R, was typically 2.58 m and the plasma minor radius, a, was 0.82 m. During the recent installation period, the inner-wall Inconel bellows cover plates were replaced with an axisymmetric inner-wall bumper limiter. This limiter is composed of water-cooled Inconel plates covered with graphite tiles, and is able to handle much more power than the moveable limiter. The inner-wall limiter defines the present large plasma dimensions to $R = 2.48$ m and $a = 0.82$ m. The full complement of protective plates was also installed.

Towards the end of the initial set of experiments with two neutral beams, a repeating pneumatic pellet injector developed at Oak Ridge National Laboratory (Combs *et al.* 1985) was installed and successfully operated to fuel the discharge. The injector was operated in deuterium to produce single 4 mm diameter (2.1×10^{21} D^0) pellets at 1300 m s^{-1}, or multiple 2.67 mm diameter (7×10^{20} D^0) pellets at up to 1350 m s^{-1}. The injector is capable of producing 4 mm pellets at 1900 m s^{-1} when operated in hydrogen. In May 1986, a more flexible eight-barrel pneumatic injector will be installed with different size pellets to optimize the fuelling-deposition profile and hence the density profile†.

3. Operating range

The operating range for large plasmas during the two neutral-beam experiments conducted on the moveable limiter is illustrated by means of the Hugill diagram shown in figure 1 where q_a is the limiter safety factor. The approach to the high-density limit is characterized by the

† See notes added in proof.

PHILOSOPHICAL TRANSACTIONS OF THE ROYAL SOCIETY A MATHEMATICAL, PHYSICAL & ENGINEERING SCIENCES

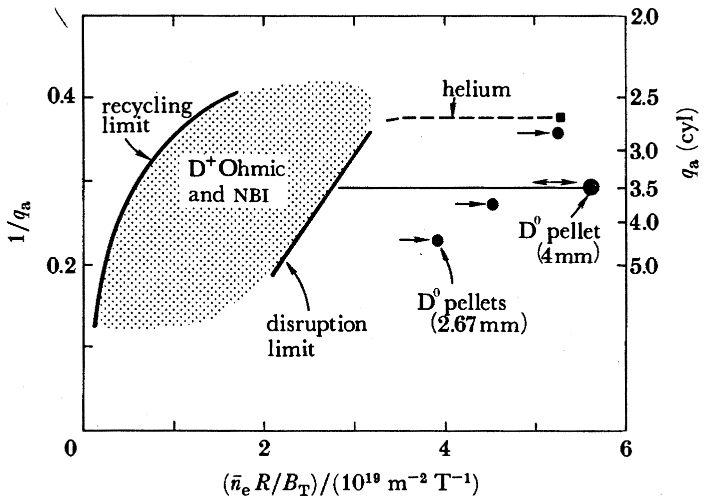

FIGURE 1. Operating range of TFTR gas-fuelled and pellet-fuelled deuterium discharges conducted on the moveable limiter. The limiter safety factor is represented by q_a.

occurrence of high edge radiation, which begins near the inner wall as a multifaceted asymmetric radiation from the edge (MARFE) (Lipschultz *et al.* 1984), and finally by high-density disruptions. In deuterium gas-fuelled discharges, the density limit corresponds to a Murakami parameter $\bar{n}_e\ R/B_t$, of *ca.* $3.2\times10^{19}\ \mathrm{m^{-2}\ T^{-1}}$. By means of pellet injection or the use of helium as the working gas, higher line-averaged densities of up to $8\times10^{19}\ \mathrm{m^{-3}}$, corresponding to a Murakami parameter of *ca.* $5.6\times10^{19}\ \mathrm{m^{-2}\ T^{-1}}$, were achieved during operation on the moveable limiter (Schmidt *et al.* 1985). Recent pellet-injection experiments on the inner wall have produced Murakami values of $6.5\times10^{19}\ \mathrm{m^{-2}\ T^{-1}}$ and a line-averaged density of $1.4\times10^{20}\ \mathrm{m^{-3}}$. Near the gas-fuelled density limit, by carefully programming the current and density waveforms, it is possible to establish stable discharges with a cold radiating mantle surrounding the plasma that isolates the hot core from contact with the limiter for many energy confinement times (Strachan *et al.* 1985). The stability of these discharges and the observation that the density limit is different for gas-fuelled and pellet-fuelled discharges suggests that the density limit is not merely defined by thermal stability due to the temperature dependence of impurity radiation as analysed previously by Gibson (1976), Rebut & Greene (1977), Ashby & Hughes (1981), Ohyabu (1979), Roberts (1983) and Perkins & Hulse (1985) but is also affected by the fuelling profile and plasma recycling.

The low-density limit is determined by recycling from the limiter and the particle confinement time. With increasing plasma current, the low-density limit increases. Thus, to obtain the low-density discharges, of particular importance in studies of the energetic-ion régime, reduced current operation has been required.

In ohmically heated discharges, Z_{eff} decreases with increasing density. According to visible bremsstrahlung and X-ray pulse-height analysis measurements, and neoclassical resistivity calculations, $Z_{\mathrm{eff}}\approx1.2$ has been achieved in high-density discharges defined by either the moveable limiter or the inner-bumper limiter. During a neutral-beam power scan at an intermediate density of *ca.* $4.6\times10^{19}\ \mathrm{m^{-3}}$ on the moveable limiter, Z_{eff} was found to increase from *ca.* 1.8 to *ca.* 2.8 with increasing power up to an injected power of 5.6 MW. Recent experiments on the inner graphite bumper limiter do not show a significant increase in Z_{eff} up to an injected power of *ca.* 11 MW (with $Z_{\mathrm{eff}}\lesssim2$) as determined by pulse-height analysis measurements and neoclassical resistivity calculations. The principal impurity is carbon, which determines both Z_{eff} and the dilution of deuterium ions, though oxygen impurities appear to plan an important role at the density limit (Dylla *et al.* 1986).

In typical high-current discharges, the most prominent type of MHD activity is sawtooth oscillations (McGuire *et al.* 1985). Sawteeth appear to play an important role in determining the temperature profile in the core of the discharge. However, they have little effect on the overall energy balance under present operating conditions (Murakami *et al.* 1986).

4. Confinement in ohmically heated discharges

Previous experiments (Hawryluk *et al.* 1984; Efthimion *et al.* 1985) at modest toroidal fields (not greater than 2.8 T) and plasma currents (not greater than 1.4 MA) demonstrated that the global energy confinement time, τ_E, scales as $\bar{n}_e\, q_a\, R^2 a$ reaching a maximum value of $\tau_E \sim 0.3$ s. Recent ohmic experiments with both gas- and pellet-fuelled discharges have concentrated on exploring the applicability of the previous scaling law over a wider operating range in density, toroidal field, and plasma current.

The analysis of the energy confinement time has relied upon the time-independent kinetic analysis code, SNAP. Figure 2 is a summary of the ohmic-heating studies for large plasmas

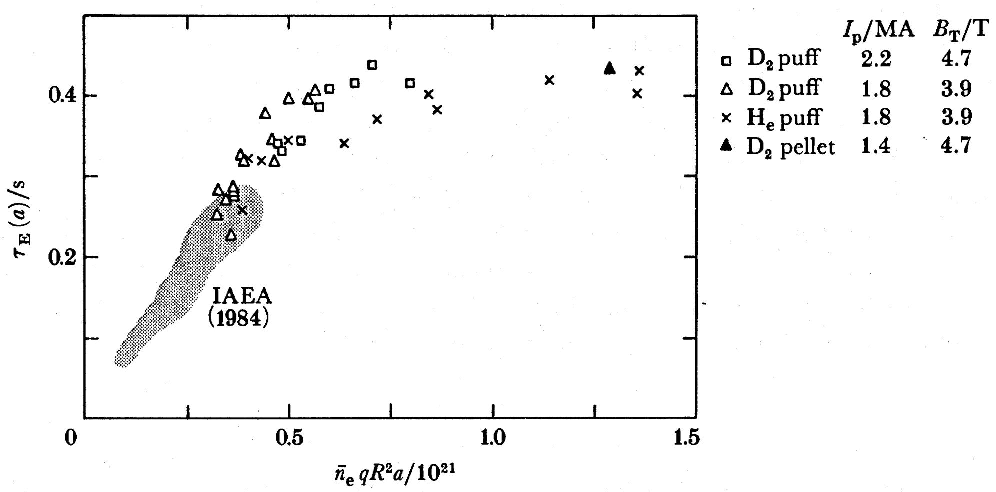

FIGURE 2. Gross energy confinement against $\bar{n}_e\, qR^2a$ for ohmically heated discharges with and without pellet injection. These experiments were performed on the moveable limiter in the large plasma configuration.

on the moveable limiter. In gas-fuelled deuterium discharges, the confinement time increases to 0.44 s, in reasonable agreement with $n_e\, q_a$ scaling for $\bar{n}_e \lesssim 4.8 \times 10^{19}\ \mathrm{m^{-3}}$. However, in both high-density helium discharges as well as high-density deuterium pellet discharges, the confinement time no longer increases linearly with line-averaged density. The roll-over in the density scaling of ohmically heated discharges is in fair agreement with the predictions of the empirical confinement model proposed by Goldston (1984), assuming that the H-mode scaling applies in these ohmic discharges. (This corresponds to multiplying the L-mode auxiliary confinement time by a factor of two.) L-mode scaling significantly underestimates both the confinement time and the density at which the transition from linear density scaling occurs. In the high-density régime, the confinement time is observed to be only a weak function of plasma current, also in fair agreement with Goldston's H-mode model. Analyses of the energy balance for helium discharges in the high-density régime, by using Thomson-scattering electron temperature profile measurements and Doppler-broadening measurements of the Ti XXI Kα line to determine the central ion temperature, indicated that the electron channel and not the ion channel is responsible for the roll-over, assuming that electron–ion heat transfer is due to Coulomb collisions. However, small systematic errors in either measurement could alter this conclusion because $(T_e - T_i)/T_e \ll 1$ so that, at present, it is not possible to exclude the possibility that ion transport is responsible for the roll-over as indicated in the Alcator-C experiments (Greenwald *et al.* 1985).

In addition to increasing the line-averaged density, pellet injection enables the formation of highly peaked density profiles. A line-averaged density of 1.4×10^{20} m^{-3} has been achieved following the injection of three 2.7 mm pellets in recent experiments conducted on the inner graphite limiter. The central electron density was 2.5×10^{20} m^{-3} and the central electron temperature was 1.25 keV as measured by Thomson scattering 400 ms after the last pellet was injected. The line-averaged density decreased to 1.1×10^{20} m^{-3} by this time. The energy confinement time was *ca.* 0.40 s according to kinematic and diamagnetic measurements corresponding to an $n_e(0)\, \tau_E \sim 1 \times 10^{20}$ m^{-3} s. The radiation loss on axis in these high density discharges due to bremsstrahlung collisions (Karzas & Latter 1961), p_b, is *ca.* 50 kW m^{-3} for a pure hydrogenic plasma. This is a significant fraction of the local ohmic input power, $p_b/p_{oh} \sim 0.2$, unlike in typical tokamak discharges. That bremsstrahlung may be important has been previously recognized. Pease (1957) pointed out the general constraints imposed on pinches when bremsstrahlung radiation equals the ohmic input power.

This peaked density profile was achieved by decreasing the plasma minor radius to 0.7 m and the plasma current to 1.6 MA to improve the pellet penetration. For a given pellet size and speed, an optimum target plasma needs to be established for adequate penetration because of the strong dependence of the ablation rate of the pellet on electron temperature. The new eight-barrel pneumatic injector with multiple pellet size and independent firing time will provide additional flexibility to optimize the deposition profile further.

5. Neutral beam scaling studies

The variation of energy confinement time with injection power of up to *ca.* 11 MW was systematically studied by operating so that the density at the end of the injection pulse was approximately constant ($\bar{n}_e \approx 4.2 \times 10^{19}$–$4.8 \times 10^{19}$ m^{-3}). These experiments were conducted in the large plasma configuration on the inner-wall limiter with deuterium gas fuelling, deuterium beams, $I_p = 2.2$ MA, and $B_T = 4.8$ T. Because there was a large power-dependent density rise due to the beam ($\Delta\bar{n}_e/\bar{n}_e$ up to *ca.* 0.7 at $P_{inj} \sim 11$ MW), the density before injection was decreased as the power increased to maintain the approximately constant final density. In this power scan, the electron and ion temperature, in ohmically heated discharges were *ca.* 2.5 keV. At $P_{inj} \approx 10$ MW, the electron temperature increased to *ca.* 4 keV according to Thomson scattering and X-ray pulse-height analysis measurements, whereas the ion temperature increased to *ca.* 5.2 keV according to Fe XXV Kα Doppler-broadening measurements. Measurements of the neutron flux by the techniques described by Hendel 1986) show that the neutron source strength increases with injected power up to *ca.* 1×10^{15} neutrons s^{-1}. The calculated neutron source strength by using the Kα Doppler-broadening measurements for the central ion temperature and assuming classical slowing down of the fast ions in gas-fuelled neutral-beam heated discharges is typically a factor of *ca.* 2 larger than the measured neutron source strength. A similar discrepancy was also observed in the compression experiments (Wong *et al.* 1985) and in gas-fuelled ohmic experiments. The reasons for the discrepancy are under investigation.

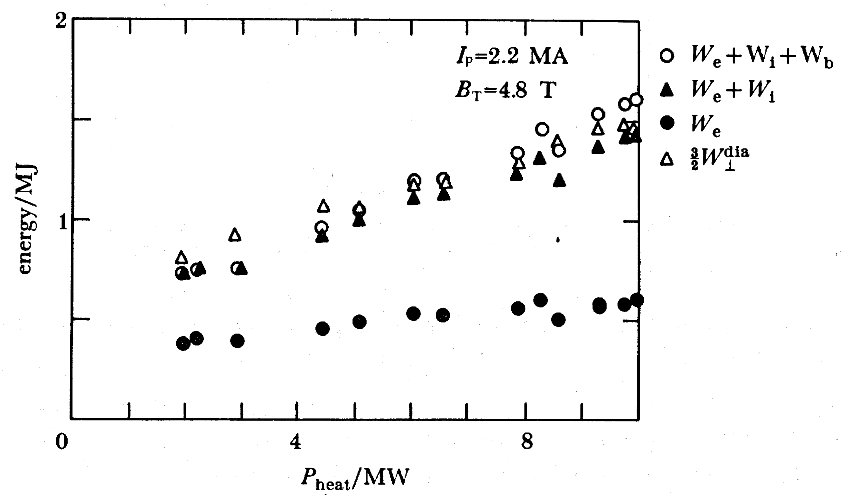

FIGURE 3. Variation of the electron, ion, and beam stored energy with heating power for the 2.2 MA power scan. Diamagnetic measurements of stored energy are shown for comparison.

Figure 3 shows the variation in the total stored energy in the thermal ions (W_i), electrons (W_e), and beam ions (W_b) with heating power (P_{heat}) for the 2.2 MA power scan. Both kinetic and diamagnetic loop measurements are shown. Because the energy stored in the beam ions is evaluated to be small, the interpretation of the diamagnetic measurements assumed the plasma was isotropic. The heating power (P_{heat}) is defined as the sum of the ohmic (P_{oh}) and the absorbed beam power (P_{abs}) after subtraction of the calculated fast-ion charge-exchange loss (P_{cx}), which is 8–16% of P_{abs} in these experiments. The stored energy increases linearly with heating power; however, the rate of increase of stored energy, dW_p/dP_{heat}, is appreciably less than the ohmic confinement time. The less-than-expected increase in stored energy is due to degradation of the global energy confinement with auxiliary heating. Previous measurements of the power radiated and the heat flux to the limiter in the standard neutral-beam heating régime are in good agreement (within $\pm 10\%$) with the ohmic- and neutral-beam-heating power (Murakami *et al.* 1985).

The gross energy confinement time $\tau_E(a)$ ($\equiv W_p/P_{heat}$ in equilibrium, where $W_p = W_e + W_i$) for the data shown in figure 3 fits the form of $\alpha + \beta/P_{heat}$ where the 'incremental' confinement time $\alpha = 0.09$ s for 2.2 MA discharges. An alternative and commonly used technique is to fit $\tau_E(a)$ by a power law dependence of $P_{heat}^{-\gamma}$, where $\gamma = 0.6$ for these data. For high-current TFTR discharges, both formulations result in similar extrapolations for $\tau_E(a)$ for when the heating power will be increased to 27 MW. Figure 4 shows the variation of $\tau_E(a)$ with power and the predictions of the empirical scaling model proposed by Goldston (1984). As mentioned above, the ohmic results are in fair agreement with the H-mode model; however, the high-power beam

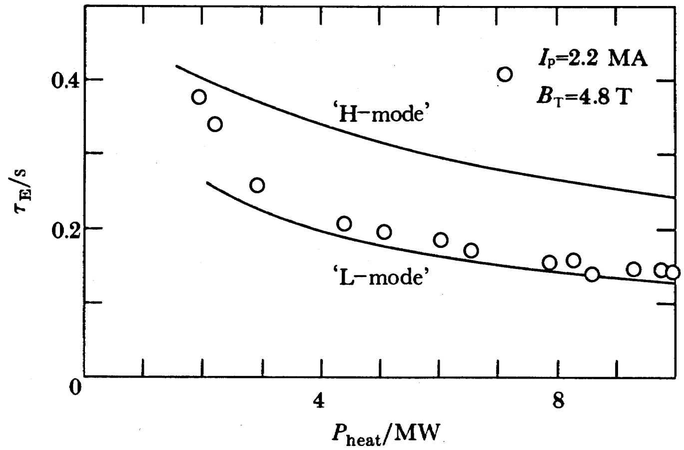

FIGURE 4. Variation of the gross energy confinement time for the power scan and comparison with L- and H-mode scaling model of Goldston (1984).

heating results are in better accord with the L-mode model. These recent results are in good agreement with the previous results reported by Murakami *et al.* (1986) on experiments conducted on the moveable limiter at the same plasma current and density. In those experiments with $P_b \leqslant 5.6$ MW, the energy confinement time was typically 10–15% greater at the same power. Figure 5 shows the favourable variation of $\tau_E(a)$ with plasma current as found in smaller tokamaks with injection (Murakami *et al.* 1986). In TFTR, variations in plasma current are typically accompanied by variations in electron density. A joint confidence analysis of the database for auxiliary heating indicates that $\tau_E(a)$ is indeed a strong function of plasma current and a weak function of density.

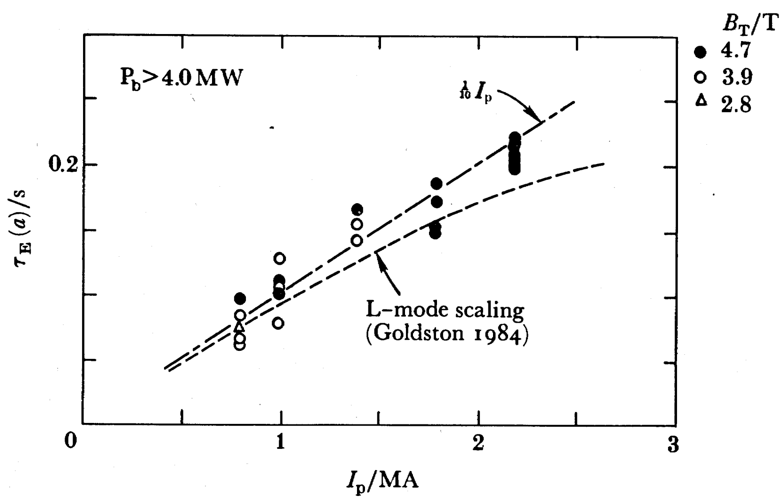

FIGURE 5. Dependence of the gross energy confinement on plasma current for experiments conducted on the moveable limiter during experiments performed with two neutral beamlines.

The degradation of confinement time with power was anticipated based on the performance of smaller tokamaks. On smaller devices, a variety of techniques have been effective in increasing the confinement time (see references in the review paper by Kaye 1985). The most successful technique has been the use of a divertor to define the plasma boundary (Keilhacker *et al.* 1985; Kitsunezaki *et al.* 1985; Fonck *et al.* 1984 and Overskei *et al.* 1984). In limited discharges, by carefully admitting low-Z impurities (Lazarus *et al.* 1984), by injecting pellets (Sengoku *et al.* 1985), or by the use of a pumped limiter on the large major radius side (Budny *et al.* 1984), enhancements in the energy confinement time have been achieved. In the upcoming series of experiments, the goal will be to extend techniques that have worked successfully on smaller devices and to develop new ones suitable for the present larger, higher-power tokamaks such as JET, TFTR, and JT-60. Though the empirical scaling models provide a useful benchmark for evaluating the efficiency of confinement enhancement techniques and device performance, the reasonable agreement between the empirical scaling models and the experimental results is not an indication of a fundamental understanding of plasma transport. This is shown by the results on smaller devices that exceeded the predictions of L-mode scaling. Indeed reproducing these enhanced confinement results on a larger machine would be a major step towards enhancing this understanding.

6. Profile variations during neutral-beam injection

The heating profile during neutral-beam injection is primarily determined by the beam energy distribution, injection angle, beam species, and plasma density profile. In comparison with the ohmic-heating profiles, which during the current flat-top are peaked on axis, the beam-heating profiles, especially with D^0 beams and high-density discharges, can be much broader and in some cases even hollow. Thus, one might expect that the shape of the temperature profile would be substantially different during neutral-beam injection. However, this is not observed.

In TFTR ohmic studies, Taylor *et al.* (1985) have shown that the electron temperature profiles are correlated with q_a. Similarly, in PDX neutral-beam heating studies, Goldston (1984) and Kaye *et al.* (1984) demonstrated that the ratio $\langle T_e \rangle / T_e(0)$, where $\langle T_e \rangle$ is the volume-averaged T_e, to be a function of $1/q_a$ independent of beam power. Figure 6 shows the *sawtooth-averaged* $\langle T_e \rangle / T_e(0)$ as a function of $1/q_a$ for TFTR discharges (Murakami *et al.* 1985*b*). In addition, the radius of the $q = 1$ surface (as determined by the soft X-ray imaging system) is also observed to be a function of $1/q_a$ for the same data independent of beam power (Murakami *et al.* 1986). These studies were conducted during the flat-top phase of the plasma current pulse in order to minimize variations in the current density profile associated with the current penetration phase and the development of the $q = 1$ surface. That both $\langle T_e \rangle / T_e(0)$ and the radius of the $q = 1$ surface are functions of $1/q_a$ suggests that there are natural profile shapes for $T_e(r)$ and possibly $q(r)$ associated with the limiter safety factor. Coppi (1980), Perkins (1984), and others have discussed the implications of a constrained temperature profile for anomalous transport. Recently, Furth (1987) and Furth *et al.* (1985) have discussed the constraints on current profile imposed by resistive kink stability requirements and their ramifications.

At present, further experiments are in progress to examine whether the current or the temperature profile is more severely constrained by q_a. In equilibrium, the current and temperature profile are related by the plasma conductivity. By applying a strong current ramp of up to 2.8 MA s^{-1} (starting at $I_p = 1.4$ MA and increasing to 2.2 MA), the current and temperature profiles have been transiently perturbed. Despite the large current ramp-up rate, the current penetration can be successfully modelled with a one-dimensional magnetic-field

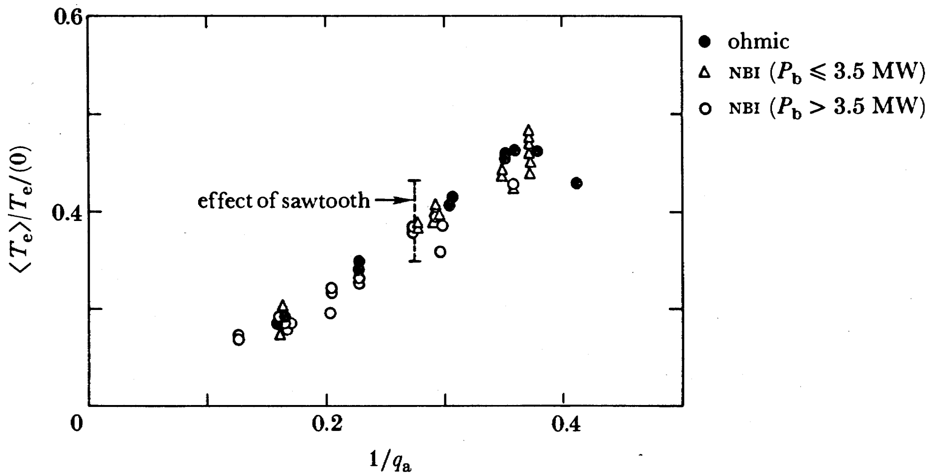

FIGURE 6. Ratio of volume-averaged electron temperature to central electron temperature as a function of the inverse of the limiter safety factor. All data points are averaged over several sawtooth periods, except the data shown by a vertical line, which are bounded by two values for the $T_e(r)$ profiles before and after a large internal disruption (sawtooth oscillation).

diffusion code, TRANSP (Hawryluk 1980), by using the measured electron-temperature profile and assuming neoclassical resistivity. Bursts of MHD activity, which occur at the highest ramp rate (typically when q_ψ is *ca.* 4), result in a significant decrease of the electron temperature in the plasma periphery which has been taken into account in the analysis. Detailed analysis of these discharges during beam injection experiments is in progress.

That the electron temperature profile shape (with electric field approximately constant across the profile) is a weak function of beam power and is similar to the ohmic temperature profile has several interesting implications because the heating profile in beam-heated discharges is different from the ohmic-heating profile. Murakami *et al.* (1985) showed that, despite shallow-beam penetration with D^0 injection, $\tau_E(a)$ values are as large as those with more penetrating H^0 injection, and that the central-core confinement is greater with D^0 injection. Similar results have been reported by Speth *et al.* (1985) on neutral-beam experiments conducted in ASDEX. These observations are similar to the T-10 electron cyclotron heating results, which showed that the confinement time remained roughly constant as the resonance layer was moved from $r = 0$ to $r \sim 0.5a$ (Alikaev *et al.* 1985). Figure 7 shows the fraction of the plasma stored energy, F_W, within $r = \frac{1}{3}a$ as a function of the fraction of the heating power, F_p, deposited within $r = \frac{1}{3}a$. In ohmic discharges, F_W increases as F_p is raised by raising q_a. With neutral-beam injection, F_p varies over a much wider range (a factor of 5); however, the variation in F_W is no broader than in the ohmic case and is determined basically by q_a rather than by F_p. Because $F_W/F_p = \tau_E(\frac{1}{3}a)/\tau_E(a)$, this indicates that the core confinement with poorly penetrating beams (in particular with pellet-fuelled beam-heated plasmas) is substantially greater than the gross energy confinement.

Schmidt *et al.* (1985), using a time-dependent kinetic analysis code, TRANSP (Hawryluk 1980, and Goldston *et al.* 1981), have shown that in the pellet-fuelled discharges the central energy confinement time $\tau_E(\frac{1}{3}a)$ is *ca.* 1 s; however, the global energy confinement is *ca.* 0.2 s, which is similar to that in lower-density gas-fuelled discharges. The results of the analysis indicate that the improvement in the central confinement time is due to a reduction in the

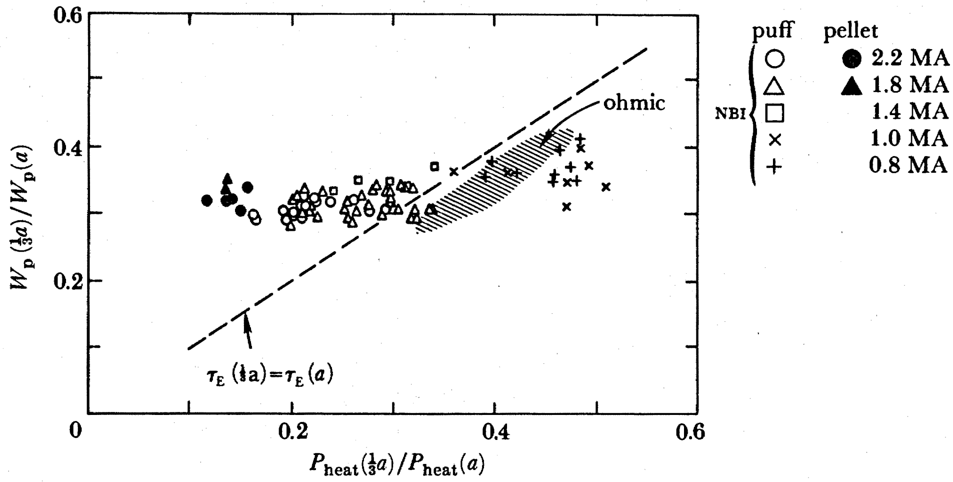

FIGURE 7. Fractional total stored energy within $r = \frac{1}{3}a$ against fractional heating power deposited within $r = \frac{1}{3}a$. The shaded area indicates a large number (*ca.* 200) of ohmically heated discharges.

thermal diffusivity and not due to a reduction in the thermal gradients (i.e. the temperature profile is largely consistent). Furth (1987) and Zweben *et al.* (1986) have pointed out that the high-density, non-centrally heated régime that can be achieved with pellet injection should lend itself to the study of alpha-heating effects. Under these conditions, the central region is expected to have a favourable $n\tau_E$ value, along with minimal levels of non-fusion background power deposition.

In these experiments the large variations in heating profile were accompanied by variations in electron density. Thus, whereas the global energy confinement was not found to vary with density, part of the variation in the central confinement time may be due to a change in the central density. Experiments are in progress to examine this by preferentially heating either the edge of the plasma or the core at constant density. This will be accomplished by choosing sources with different tangency radii. The temporal evolution of these edge-heated discharges may also enable us to examine whether an inward heat pinch is present. An inward heat pinch would affect the conventional thermal diffusion analysis that was used to analyse the pellet-fuelled discharges. Direct edge heating can also be used to test the hypothesis proposed by Rebut & Hugon (1985) about local heating against power radiated in determining the stability of magnetic islands.

7. Major-radius compression experiments

Compression experiments in which the plasma major radius was reduced from 3.0 to 2.1 m in *ca.* 20 ms have been performed in TFTR. In an initial series of experiments, Tait *et al.* (1985) observed that the increase in $T_e(0)$ was less than theoretically expected, though the discrepancy in $n_e(0)$ scaling was less. Further experiments and analysis (Kiraly *et al.* 1985) indicate that high-frequency MHD activity during compression as well as the occurrence of an exceptionally large internal disruption (sawtooth oscillation) may be important to the understanding and interpretation of these results. Additional experiments are planned to clarify the role of MHD activity and to evaluate transport during compression. During the two-neutral-beam run period, acceleration of beam ions was studied in 450 kA discharges that were compressed from 3.0 m to 2.17 m in *ca.* 15 ms. The tangentially coinjected deuterium beam ions were accelerated from 82 to 150 keV in good agreement with Fokker–Planck simulations as shown in figure 8 (Wong *et al.* 1985; Kaita *et al.* 1986). Measurements of the neutron emission from d(d, n)^{3}He

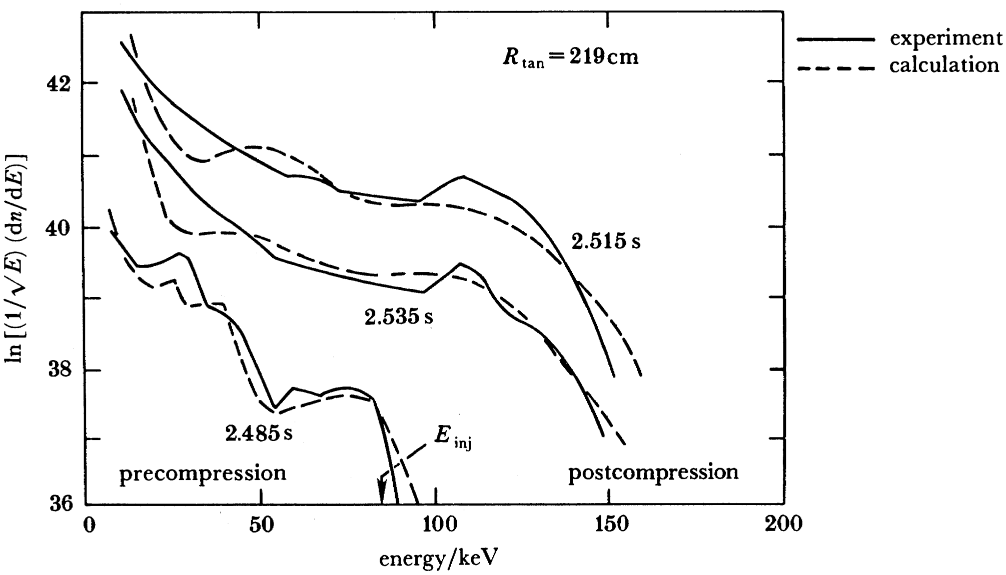

FIGURE 8. Charge exchange measurements of the fast-ion slowing-down spectra before and after major-radius compression commencing at 2.5 s. The dashed curves are Fokker–Planck simulations.

reactions and of 15 MeV protons from ^{3}He(d, p)α reactions show a substantial enhancement of the plasma reactivity as expected. Future effort on plasma compression will focus on utilizing it as a tool to understand plasma transport during the intense auxiliary heating that occurs during compression.

8. Energetic ion mode

Operation of TFTR at low I_p (0.4–1.0 MA) and high beam power has allowed access to a very-low-density régime ($\bar{n}_e \sim 1 \times 10^{19}$ m^{-3}) characterized by high values of ion temperature and toroidal rotation velocity. In this régime, the density rise saturates during injection and the overall density increase is much less than the integrated number of beam ions injected into the torus. The reduced density rise together with the lower initial density is required for operation in this régime. The dependence of the uncorrected ion temperature measurements (from Ti XXI Kα Doppler broadening and near-perpendicular passive hydrogen charge-exchange analysis) on absorbed beam power normalized by line-averaged density is shown in figure 9. Substantial corrections to both ion temperature measurements are calculated. The impurity-ion temperatures need to be corrected for the preferential coupling of the beam power to the impurity ions (Eubank *et al.* 1979). In addition, smaller corrections due to the emission profile and the shear in the toroidal velocity affect these measurements. The charge exchange measurements are corrected for emission profile, plasma opacity and the high toroidal velocity. Central hydrogen temperatures up to 9 ± 2 keV have been achieved. The ion heating efficiency, $\eta_i = \Delta T_i \bar{n}_e / P_{\text{abs}}$, in this régime is similar to that in the standard régime (Medley *et al.* 1985).

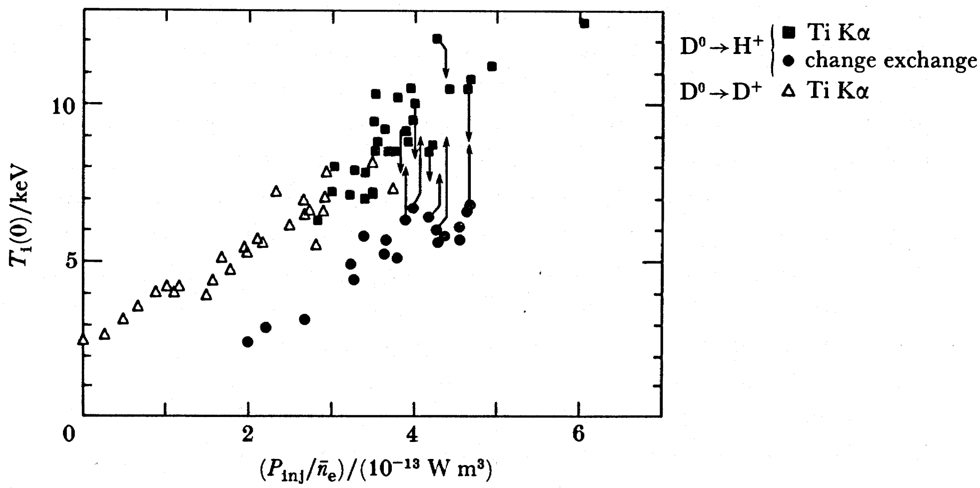

FIGURE 9. Dependence of the uncorrected ion temperature measurements based on Doppler broadening of T_i Kα lines and perpendicular charge-exchange spectra $[T_i(cx)]$ as a function of $P_{inj}/\bar{n}_e$. The correction to the measurements is shown by the arrows.

The central toroidal velocity is measured by the Doppler shift of the Tixxi Kα line and increases linearly with $P_{inj}/\bar{n}_e$ to 7×10^5 m s^{-1} as shown in figure 10. This corresponds to a ratio of $V_\phi(0)/v_H \equiv V_\phi(0)/(T_i/m_H)^{\frac{1}{2}} \approx 0.6$. At modest values of $P_{inj}/\bar{n}_e$, measurements of the toroidal velocity using the $m = 1$ sawtooth precursor are in good agreement with the Ti Kα-line Doppler-shift measurements. At high power, sawteeth and the $m = 1$ precursor are not observed.

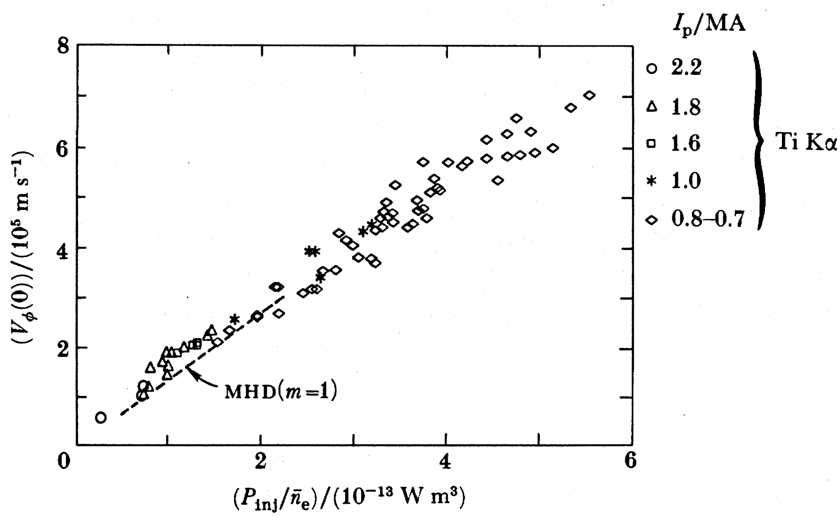

FIGURE 10. Central toroidal rotation velocity as a function of the ratio of injected beam power to line-averaged electron density.

During neutral-beam injection, the surface voltage decreases substantially. Experiments utilizing three cobeamlines have resulted in negative surface voltages ($V_s \approx -0.15$ V) with P_{inj} of *ca.* 8 MW in a 700 kA discharge with $\bar{n}_e = 2 \times 10^{19}$ m^{-3}. The surface voltage at the end of the injection pulse decreases with increasing power and increases with increasing current. TRANSP analysis and BALDUR simulation, which do not yet include the effects of plasma rotation, predict a neutral beam driven current of 300–500 kA with $P_{\text{inj}} \sim 5$ MW. A more quantitative comparison between theory and experiment requires the inclusion of plasma rotation in the time-dependent analysis. The usual assumption that the plasma motion is negligible compared with the fast-ion velocity is not adequate in this régime, substantially complicating the analysis of these discharges (Goldston 1985). Inclusion of these effects in the time independent code, SNAP, results in a significant reduction in the beam density, a reduction in direct beam heating, and the addition of viscous heating. Further work on evaluating the effects of rotation is in progress. Despite a large population of beam ions and high toroidal velocity, the behaviour of the ion heating, momentum confinement, and global energy confinement is similar to that observed in the standard neutral-beam heating régime. With the addition of a beamline oriented in the counterdirection, the effects of plasma rotation and beam current drive on confinement will be readily studied. Furthermore, in this configuration, substantial enhancements in neutron production from collisions between co- and counter-streaming fast ions are expected, especially if tritium and deuterium beams are used simultaneously.

9. Conclusions

The difficult problems associated with making high-field, high-current, high-electron density, and high-purity discharges have been successfully resolved in TFTR. Ohmic discharges spanning a wide range of operating parameters provide a variety of interesting target plasmas for neutral beam injection. Pellet injection can create target plasmas with exceptionally high central densities and long energy confinement times. The initial neutral-beam-heating experiments with two beamlines have further expanded the operating parameters. During the next phase of operation, the emphasis will be to gain a better understanding of the transport properties to optimize the energy confinement time. Techniques for the enhancement of τ_E that would be effective at high power in a large undiverted tokamak could have a significant impact on the design of future DT reactors. Experiments in the low-density energetic-ion régime offer an alternative approach to achieving $Q \sim 1$ and are of basic physics interest. The acceleration of beam ions during compression has been demonstrated to increase the plasma reactivity as expected. The four large tokamaks, JET, JT-60, and TFTR, which are now in operation and T-15, which is under construction, have been optimized differently. Their roles in the advancement of fusion research are quite distinctive and each device will be able to make a unique contribution.

We are grateful to D. J. Grove, H. P. Furth, P. H. Rutherford and J. R. Thompson for their advice and support, and J. Strachan and W. Heidbrink for useful discussions. This work was supported by US DOE Contract No. DE-AC02-76-CH03073. The ORNL participants were also supported by US DOE Contract No. DE-AC05-840R21400 with Martin Marietta Energy Systems, Inc.

MATHEMATICAL, PHYSICAL & ENGINEERING SCIENCES
THE ROYAL SOCIETY A
PHILOSOPHICAL TRANSACTIONS OF

References

Alikaev, V. V. *et al.* 1985 In *Proc. 10th Int. Conf. Plasma Physics and Controlled Nuclear Fusion Research, London, 12–19 September 1984, vol. 1*, pp. 419–432. Vienna: IAEA.

Ashby, D. E. T. F. & Hughes, M. H. 1981 *Nucl. Fusion* **21**, 911–926.

Budny, R. *et al.* 1984 *J. nucl. Mater.* **121**, 294–303.

Combs, S. K. *et al.* 1985 *Rev. scient. Instrum.* **56**, 1173–1178.

Coppi, B. 1980 *Comments Plasma Phys. controlled Fusion* **5**, 261–269.

Dylla, H. F. 1986 Princeton Plasma Physics Laboratory Report no. 2307. (Also *J. Vac. Sci. Technol* (In the press).)

Efthimion, P. C. *et al.* 1984 *Phys. Rev. Lett.* **52**, 1492–1495.

Efthimion, P. C. *et al.* 1985 In *Proc. 10th Int. Conf. Plasma physics and Controlled Nuclear Fusion Research, London, 12–19 September 1984, vol. 1*, pp. 29–44. Vienna: IAEA.

Eubank, H. P. *et al.* 1979 In *Proc. 10th Int. Conf. Plasma Physics and Controlled Nuclear Fusion Research, London, 12–19 September 1984, vol. 1*, pp. 167–198. Vienna: IAEA.

Eubank, H. P. *et al.* 1985 In *Proc. 10th Int. Conf. Plasma Physics and Controlled Nuclear Fusion Research, London, 12–19 September 1984, vol. 1*, pp. 303–318. Vienna: IAEA.

Fonck, R. J. *et al.* 1984 In *Proc. 4th International Symposium on Heating in Toroidal Plasmas, Rome, 1984* vol. 1, pp. 37–56. Frascatti: ENEA.

Furth, H. P. *et al.* 1985 In *Proc. 12th European Conference on Controlled Fusion and Plasma Physics, Budapest 2–6 September 1985*. (*Europhysics Conference abstracts* **9F** (2), 358–361.)

Furth, H. P. 1987 In *Proc. Workshop on Basic Physical Processes of Toroidal Fusion Plasmas, Varenna, Italy, 26–31 August 1985* (In the press.)

Gibson, A. 1976 *Nucl. Fusion* **16**, 546–550.

Goldston, R. J. *et al.* 1981 *J. Comput. Phys.* **43**, 61–78.

Goldston, R. J. 1984 *Plasma Phys. controlled Fusion* **26**, 87–99.

Goldston, R. J. 1985 In *Proc. Workshop on Basic Physical Processes of Toroidal Fusion Plasmas, Varenna, Italy, 26–31 August, 1985* (In the press.)

Greenwald, M. *et al.* 1985 In *Proc. 10th Int. Conf. Plasma Physics and Controlled Nuclear Fusion Research, London, 12–19 September 1984*, vol. 1, pp. 45–55. Vienna: IAEA.

Hawryluk, R. J. 1980 In *Proc. Course in Physics Close to Thermonuclear Conditions Varenna, Italy*, report EUR-FU-BRU/XII/476/80, pp. 503–531.

Hawryluk, R. J. *et al.* 1984 In *Proc. 4th International Symposium on On Heating in Toroidal Plasmas, Rome* (*Inter. School of Plasma Physics, Varenna*) pp. 1012–1032.

Hendel, H. W. 1986 *IEEE Trans. Nucl. Sci.* **33**, 670–674.

Jassby, D. L. 1977 *Nucl. Fusion* **17**, 309–363.

Johnson, L. C. & Young, K. M. 1988 In *Proc. Course on Diagnostics for Fusion Reactor Conditions Varenna* (*Como*), *Italy, 6–17 September 1982*, vol. 2, pp. 551–571. New York: Pergamon Press.

Kaita, R. *et al.* 1986 Princeton Plasma Physics Laboratory Report no. 2321. (Also *Nucl. Fusion* (Submitted.).)

Karzas, W. J. & Latter, R. 1961 *Astrophys. J. Suppl.* **6**, 167–212.

Kaye, S. M. 1985 *Phys. Fluids* **28**, 2327–2343.

Kaye, S. M. *et al.* 1984 *Nucl. Fusion* **24**, 1303–1334.

Keilhacker, M. *et al.* 1985 In *Proc. 10th Int. Conf. Plasma Physics and Controlled Nuclear Fusion Research London, 12–19 September 1984*, vol. 1, pp. 71–85. Vienna: IAEA.

Kiraly, J. *et al.* 1985 Princeton Plasma Physics Laboratory Report no. 2254.

Kitsunezaki, A. *et al.* 1985 In *Proc. 10th Int. Conf. Plasma Physics and Controlled Nuclear Fusion Research London, 12–19 September 1984*, vol. 1, pp. 57–66. Vienna: IAEA.

Lazarus, E. A. *et al.* 1984 *J. Nucl. Mater.* **121**, 61–68.

Lipschultz, B. *et al.* 1984 *Nucl. Fusion* **24**, 977–988.

Medley, S. S. *et al.* 1985 In *Proc. 12th European Conference on Controlled Fusion and Plasma Physics, Budapest, Hungary, 2–6 September 1985*. (*Europhysics Conference abstracts* **9F** (1), pp. 343–346.)

McGuire, K. *et al.* 1985 In *Proc. 12th European Conference on Controlled Fusion and Plasma Physics, Budapest, Hungary, 2–6 September 1985* (*Europhysics Conference abstracts* **9F** (1), pp. 134–137).

Mueller, D. *et al.* 1986 Discharge Control and Evolution in TFTR. In *Proc. 7th Course of the International School of Fusion Reactor Technology Erice, Italy, July 1985*, pp. 143–157. New York: Plenum Publishing Corporation.

Murakami, M. *et al.* 1985 Proc. 6th Topical Meeting on the Technology of Fusion Energy, San Francisco, March 1985. *Fusion Technol.* **8**, 657–663.

Murakami, M. *et al.* 1986 In *Proc. 12th European Conference on Controlled Fusion and Plasma Physics, Budapest, 2–6 September 1985*. (*Plasma Phys. controlled Fusion* **28**, 17–27.)

Ohyabu, N. 1979 *Nucl. Fusion* **19**, 1491–1497.

Overskei, D. *et al.* 1984 In *Proc. 4th International Symposium on Heating in Toroidal Plasmas, Rome 1984*, vol. 1, pp. 21–36. Frascatti: ENEA.

Pease, R. S. 1957 *Proc. phys. Soc.* B **70**, 11–23.

Perkins, F. W. 1984 In *Proc. 4th International Symposium on Heating in Toroidal Plasmas, Rome* (International School of Plasma Physics, Varenna) pp. 977–988.
Perkins, F. W. & Hulse, R. A. 1985 *Phys. Fluids* **28**, 1837–1844.
Rebut, P. H. & Greene, B. J. 1977 In *Plasma Physics and Controlled Nuclear Fusion Research, Berchtesgarten, 6–13 October 1976*, vol. 2, pp. 3–16. Vienna: IAEA.
Rebut, P. H. & Hugon, M. 1985 In *10th Int. Conf. on Plasma Physics and Controlled Nuclear Fusion Research, London, 12–19 September 1984*, vol. 2, pp. 197–212. Vienna: IAEA.
Roberts, D. E. 1983 *Nucl. Fusion* **23**, 311–329.
Schmidt, G. L. *et al.* 1985 In *Proc. 12th European Conference on Controlled Fusion and Plasma Physics, Budapest, 2–6 September 1985.* (*Europhysics conference abstracts* **9F** (2), 674–677.)
Sengoku, S. *et al.* 1985 In *10th Int. Conf. Plasma Physics and Controlled Nuclear Fusion Research London, 12–19 September 1984*, vol. 1, pp. 405–415. Vienna: IAEA.
Speth, E. *et al.* 1985 In *Proc. 12th European Conference on Controlled Fusion and Plasma Physics, Budapest, 2–6 September 1985.* (*Europhysics conference abstracts* **9F** (2), 284–287.)
Strachan, J. D. *et al.* 1985 In *Proc. 12th European Conference on Controlled Fusion and Plasma Physics, Budapest, 2–6 September 1985.* (*Europhysics conference abstracts* **9F** (2), 339–342.)
Tait, G. *et al.* 1985 In *Proc. 10th Int. Conf. on Plasma Physics and Controlled Nuclear Fusion Research London, 12–19 September 1984*, vol. 1, pp. 141–154. Vienna: IAEA.
Taylor, G. *et al.* 1985 Princeton Plasma Physics Laboratory Report no. 2221. (Also *Nucl. Fusion* **26** (1986).)
Wong, K. L. *et al.* 1985 *Phys. Rev. Lett.* **55**, 2587–2590.
Zweben, S. J., Redi, M. H. & Bateman, G. 1986 Princeton Plasma Physics Laboratory Report no. 2316.

Notes added in proof (*January 1987*)

1. The improved species mix sources were installed in December 1986 and January 1987. Full parameters will be achieved at the end of 1987.

2. The pellet injector was installed in May 1986 and is operational.

PHILOSOPHICAL TRANSACTIONS OF THE ROYAL SOCIETY A MATHEMATICAL, PHYSICAL & ENGINEERING SCIENCES